Optik - International Journal for Light and Electron Optics 173 (2018) 132–138

Contents lists available at ScienceDirect

Optik

journal homepage: www.elsevier.com/locate/ijleo

Original research article

Computational design of high efficiency a-Si:H/CIGS monolithic tandem solar cell

Sunhwa Lee[a], Sangho Kim[b], Youngkuk Kim[a], Jinjoo Park[a,*], Junsin Yi[a,b,*]

[a] School of Information and Communication Engineering, Sungkyunkwan University, Suwon 16419, Republic of Korea
[b] Department of Energy Science, Sungkyunkwan University, Suwon 16419, Republic of Korea

ARTICLE INFO

Keywords:
Tandem
a-Si:H
CIGS
Thin film solar cell
Simulation

ABSTRACT

In this work, we investigate numerical simulations of single junction hydrogenated amorphous silicon solar cells (a-Si:H), Cu (In, Ga) Se_2 (CIGS) solar cells, and tandem solar cells with a-Si:H as the top cell and (CIGS) as the bottom cell using an advanced semiconductor analysis program. The optical bandgaps and thicknesses of the tandem solar cell were studied to optimize current matching. The tunnel-recombinaton (TJ) junctions were studied with different structures. The optimal structure was investigated using the optimal TJ junction, which consists of p-type microcrystalline silicon, n-type nanocrystalline silicon and AZO. The characteristics of the optimal a-Si:H/CIGS solar cell were a short circuit current density of 17.57 mA/cm^2, and an open circuit voltage of 1.67 V. These results can be used as a basis for effectively developing low-cost and high-efficiency solar cells.

1. Introduction

Many studies have been conducted to improve the efficiency of single junction solar cells which is already close to the theoretical efficiency limit [1]. Many attempts have been made to fabricate multi-junction solar cells using thin film solar cells to reduce costs and overcome the efficiency limitation of single junction solar cells. Multi-junction solar cells can achieve higher conversion efficiencies because they reduce the energy loss through materials with different bandgaps and they absorb a wider range of solar irradiation. Thin film solar cells have been developed using various materials, such as hydrogenated amorphous silicon (a-Si:H), Cu (In,Ga)Se_2 (CIGS), CdTe, and III-V and organic materials [2–5]. Research on tandem solar cells using a-Si:H and III-V solar cells has been carried out [6–9]. CIGS tandem solar cells posed difficulties in previous studies, even though they offered easy band gap control and excellent optical absorption characteristics [10–12]. When using a CIGS solar cell as the bottom cell and a chalcopyrite based top cell with a wide band gap, Ag(In,Ga)Se_2 (AIGS) and $CuGaSe_2$ (CGS), the efficiency was decreased [13,14]. This is because of the high process temperature required for the formation of the top cell, which causes problems in the bottom cell junction. Recently, a hybrid tandem solar cell using a perovskite cell as the top cell and a CIGS cell as the bottom cell has been studied to solve the process problem [15]. However, perovskite cells still cause stability issues. Another approach for demonstrating to use of tandem solar cells is to combine a top a-Si:H solar cell with a bottom CIGS solar cell. The efficiency and stability of the a-Si:H solar cell has been verified and this cell does not affect the bottom CIGS cell because it requires a low process temperature, which can be as low as 200 °C [16].

In this study, we present simulation results for tandem solar cells using an a-Si:H top cell and a CIGS bottom cell using an advanced semiconductor analysis (ASA) program. First, a single junction simulation of an a-Si:H cell and a CIGS cell was performed.

* Corresponding authors at: School of Information and Communication Engineering, Sungkyunkwan University, Suwon 16419, Republic of Korea.
E-mail addresses: jwjh3516@skku.edu (J. Park), Junsin@skku.edu (J. Yi).

https://doi.org/10.1016/j.ijleo.2018.08.004
Received 7 June 2018; Received in revised form 3 August 2018; Accepted 4 August 2018

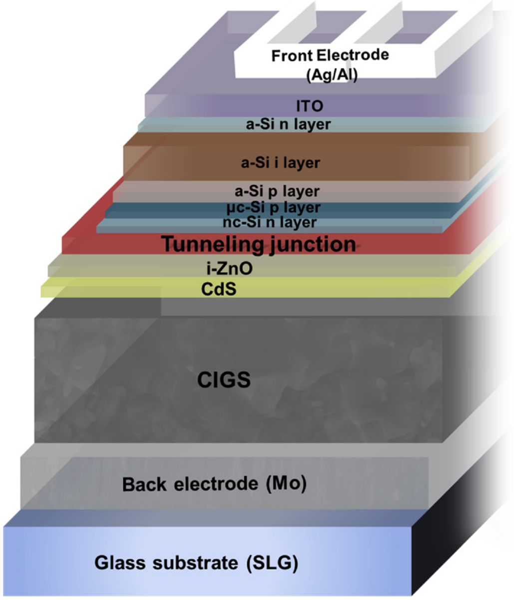

Fig. 1. Device structure of an a-Si:H/CIGS tandem solar cell.

We performed band gap engineering of the top and bottom cells for current matching. We also simulated the most important tunnel-recombination (TJ) layer in tandem solar cell. We simulated aluminum doped zinc oxide (AZO), p-type microcrystalline silicon (p-uc-Si) and n-type nanocrystalline silicon (n-nc-Si) as TJ layers. These simulations were carried out to identify essential factors for achieving effective TJ junction.

2. Numerical simulation

The ASA program developed at Delft University of Technology was used to develop the numerical simulations for the proposed a-Si:H/ CIGS tandem solar cell. The structure of the a-Si:H/CIGS tandem solar cell is shown in Fig. 1. It consists of an a-Si:H top cell and a narrow bandgap CIGS bottom cell. The ASA program can solve basic semiconductor equations including the Poisson equation and the continuity equations for electrons and holes:

$$\mathrm{div}\ (\varepsilon\ \mathrm{grad}\ \psi) = -\rho \tag{1}$$

$$\frac{\partial n}{\partial t} = \frac{1}{q} divJ_n + G_{opt} - R_{net} \tag{2}$$

$$\frac{\partial p}{\partial t} = -\frac{1}{q} divJ_n + G_{opt} - R_{net} \tag{3}$$

Where, ε is the permittivity of the semiconductor, ψ is the electrostatic potential with reference to the vacuum level, ρ is the space charge density, J_n (J_p) is the electron (hole) current density, G_{opt} is the optical generation rate, R_{net} is the net concentration and $\frac{\partial n}{\partial t}$ ($\frac{\partial p}{\partial t}$) is time rate change in the electron (hole) concentration. The Shockely-Read-Hall (SRH) recombination model was used to calculate carrier recombination rates which depend on the density of states present within the band gap, the defect energy level and the electron and hole capture cross sections. The Gaussian defect distribution was used in the standard model to describe the defect states of the CIGS bottom cell. To simulate the a-Si:H top cell, we used a defect-pool model (DPM) with valence band tail and conduction band tail states. The material parameters used in the simulation are shown in the Table 1.

3. Results and discussion

3.1. Sub-cell simulations

Simulation of the a-Si: H solar cell according to the optical bandgap of the absorber layer were performed. These simulations were performed using optical data (reflectance index, n, and extinction coefficient, k) obtained via ellipsometry. Table 2 shows the J-V parameters of the a-Si:H cell used as the top cell. As the optical band gap of absorber layer increases, the short circuit current density (J_{sc}) decreases. It is because the wavelength range that can be absorbed by the increased bandgap is reduced. The intrinsic a-Si:H thin film used as an absorber layer can be used to control the optical bandgap via tuning of certain process conditions, such as the SiH_4 and H_2 gas flow rate, pressure and power. As the bonding configuration in the layer is changed, properties such as defect density also

Table 1
Input parameter for ASA simulation.

Layer Parameters	Solar cell layers			
	AZO	i-ZnO	CdS	CIGS
L (nm)	50	50	50	2500
$m_{u.e}$ (μ_e) (cm^2/Vs)	50	50	10	300
$m_{u.h}$ (μ_h) (cm^2/Vs)	5	5	1	3
E_g (eV)	3.30	3.30	2.40	variable
chi (χ) (eV)	4.00	4.00	4.50	4.7
nc (m^{-3})	2.2E+24	2.2E+24	2.2E+24	2.2E+24
nv (m^{-3})	1.8E+25	1.8E+25	1.8E+25	1.8E+24
n (m^{-3})	5.0E+22		5.0E+23	1.0E+23
ε_r	9	9	10	13.6
dbond				
Nd (m^{-3})			1E+22	3.0E+22
e.corr (eV)	0.2	0.2	0.4	0.4
ce.neut	0.7E-15	1.0E-15	1.0E-14	2.0E-14
ce.pos	7E-15	50E-15	1.0E-14	2.0E-14
ch.neut	0.7E-15	1.0E-15	5.0E-12	1.0E-11
ch.neg	7E-15	100E-15	5.0E-12	1.0E-11

Table 2
The J-V parameter of a-Si:H and CIGS single solar cell with different optical bandgap.

		J_{sc} (mA/cm^2)	V_{oc} (mV)	FF (%)	Eff (%)
Top	1.72	19.37	857	80.90	13.43
	1.74	19.1	862	80.72	13.29
	1.76	18.51	868	80.54	12.94
	1.78	18.08	874	80.24	12.68
	1.82	16.91	885	78.98	11.82
Bottom	1.2	37.32	575	72.00	15.45
	1.3	34.65	675	73.92	17.29
	1.4	31.98	768	76.14	18.7
	1.5	29.41	864	77.84	19.78
	1.6	25.89	958	78.90	19.57

change [16]. To increase the current density of the short wavelength region, a wide bandgap material such as a-SiO_x:H or a-SiC:H should be used as the window layer. In this simulation, the J_{sc} was increased in the short wavelength region using an a-SiO_x:H n-layer and a J_{sc} value of approximately 17–20 mA/cm^2 and the open circuit voltage (V_{oc}) of about 900 mV was obtained.

A simulation of the CIGS cell used as the bottom cell was performed. The CIGS materials are known to have a high absorption coefficient. The simulation was carried out through the optical data found in the literature [17]. The optical bandgap of CIGS layer varies from 1.011 to 1.68 eV depending on their composition. They have an optical bandgap of 1.011 eV for CIS and 1.68 eV for CGS [18,19]. Table 2 shows the J-V curves for various optical bandgap. As the optical bandgap increases, the absorbable wavelength region shifts to the short wavelength. The built-in voltage (V_{bi}) was increased due to the high optical bandgap. J_{sc} decrease from 37.32 mA/cm^2 to 25.89 mA/cm^2, and V_{oc} increase from 575 mV to 958 mV.

3.2. Tandem cell simulations

The a-Si:H/CIGS tandem solar cell structure that was simulated is shown in Fig. 1. The J-V parameters of the tandem cell are shown in Fig. 2(a) for various optical bandgap of the a-Si:H top cell. The absorber layer thickness of the top cell is 550 nm and optical band gap of bottom cell is 1.2 eV. The efficiency of the tandem cell is affected by the J_{sc}. J_{sc} changes according to the current matching between the top cell and the bottom cell. As the optical bandgap of the absorber layer of the top cell increases, J_{sc} decreases owing to current density reduction occurring in the top cell as shown in the single cell simulation results. Fig. 2(b) shows the J-V parameter according to the thickness of the absorber layer of the top cell. The optical band gap of the top cell is 1.72 eV and bottom cell is 1.2 eV. As the thickness of the absorber layer increases, the fill factor (FF) decreases because of the decrease of the electric field in the top cell. J_{sc} increases from 15.14 mA/cm^2 to 18.26 mA/cm^2 as the absorber layer thickness of top cell increases from 250 nm to 650 nm. The absorber layer of the top cell affects the short wavelength region. The J-V parameters of the tandem cell are shown in Fig. 2(c) with the variation of optical band gap of CIGS bottom cell. The absorber layer thickness of the top cell is 550 nm and optical band gap is 1.72 eV. As the optical bandgap of the bottom cell increases, V_{oc} increases from 1.407 V to 1.77 V. However, J_{sc} decreases from 18.27 mA/cm^2 to 9.11 mA/cm^2. In single CIGS cells, the highest efficiency was obtained at a bandgap of 1.4 eV, whereas the highest efficiency was obtained at a bandgap of 1.3 eV for the tandem cell. Generally, when the top cell has a bandgap of 1.7–1.8 eV,

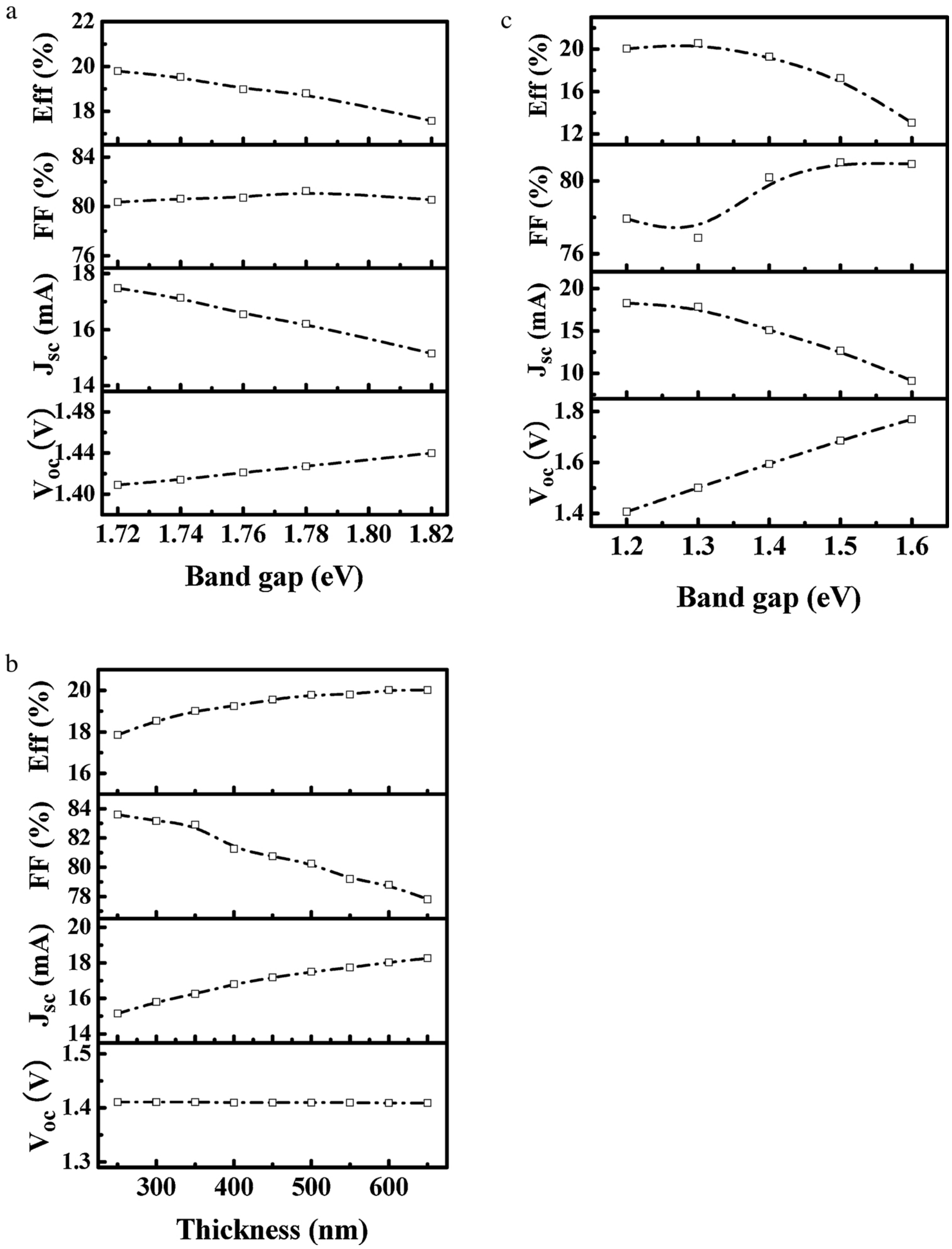

Fig. 2. Simulated J-V parameters of an a-Si:H/CIGS tandem solar cell with (a) different optical bandgaps of the top cell and (b) different thicknesses of the top cell absorber layer and (c) different optical bandgaps of the bottom cell.

the bandgap of the bottom cell has the highest efficiency at 1.12 eV. As the bandgap of the bottom cell decreases, J_{sc} increases but V_{oc} also sharply decreases, resulting in a decrease in efficiency. It is important to derive the trade-off point between J_{sc} and V_{oc} in the tandem cell. The current matching simulation results obtained via variations of the optical bandgap and thickness of the top cell and the optical bandgap of bottom cell are shown in Fig. 3. Since the thickness of the bottom cell does not significantly affect the J_{sc}, CIGS cell optimized thickness of 2.5um was used. The current density mismatch still occurs when the absorber layer thickness and optical band gap of the top cell are varied. The simulation indicates that the efficiency would be optimal at $Eg_{\text{ Bottom,abs}} = 1.3$ eV. The simulation results for the TJ layer was shown, which plays the most important role in the tandem cell. The simulation was performed using TJ layers of AZO, p-uc-Si/AZO, n-nc-Si/AZO and p-uc-Si/n-nc-Si/AZO. The simulated J-V parameters are listed in Table 3 for the different TJ layers. The tandem junction was formed when the p-uc-Si/n-nc-Si/AZO TJ layers were used. When the other TJ layers were used, the results were similar to those obtained with a single cell. The optimized J-V curve of sub cell and tandem cell was shown in Fig. 4. The a-Si:H solar cell has a higher V_{oc} but lower J_{sc} and CIGS solar cell has a higher J_{sc} but lower V_{oc}. The tandem cell J_{sc} is 17.57 mA/cm^2 and V_{oc} is 1.665 V. The optimized efficiency of tandem cell is 23.32%. We associated these varied cell results

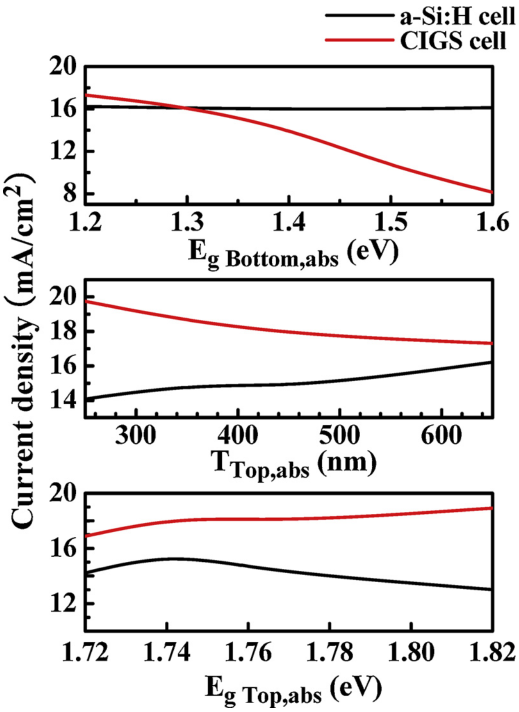

Fig. 3. Current density of the top and bottom cell as a function of optical bandgap and thickness of the top cell and optical bandgap of the bottom cell.

Table 3
The J-V parameter of a-Si:H/CIGS tandem solar cell with different TJ layer.

	J_{sc} (mA/cm^2)	V_{oc} (mV)	FF (%)	Eff (%)
AZO	17.66	680	64.20	7.71
p-uc-Si/ AZO	17.66	689	55.97	6.81
n-nc-Si/ AZO	17.66	766	61.06	8.26
p-uc/n-nc-Si/ AZO	17.57	1665	79.72	23.32

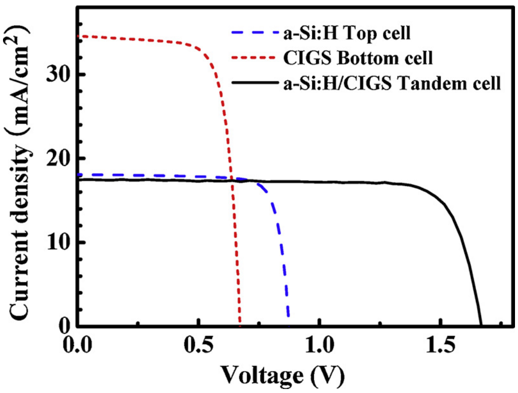

Fig. 4. J-V curve of a-Si:H sub cell, CIGS sub cell and a-Si:H/CIGS tandem solar cell.

with the band structure near the TJ region. In order to form a tandem junction, the carriers formed on the top and bottom cells should be recombined in the TJ layer. Our simulation results show the effects of the TJ layers with the band diagram, the electric field and the recombination rate on the tandem solar cell. Fig. 5 shows the band diagram of the tandem cell under thermal equilibrium conditions for the different TJ layers. The holes from the valence band of the top cell and the electrons from the conduction band of the bottom cell recombine in the TJ layers. When AZO was used as a TJ layer, the valence band offset between the p-a-Si:H layer and the AZO layer was large and acted as a barrier (Fig. 5(a)). When p-uc-Si/AZO was used, a larger valence band offset formed between

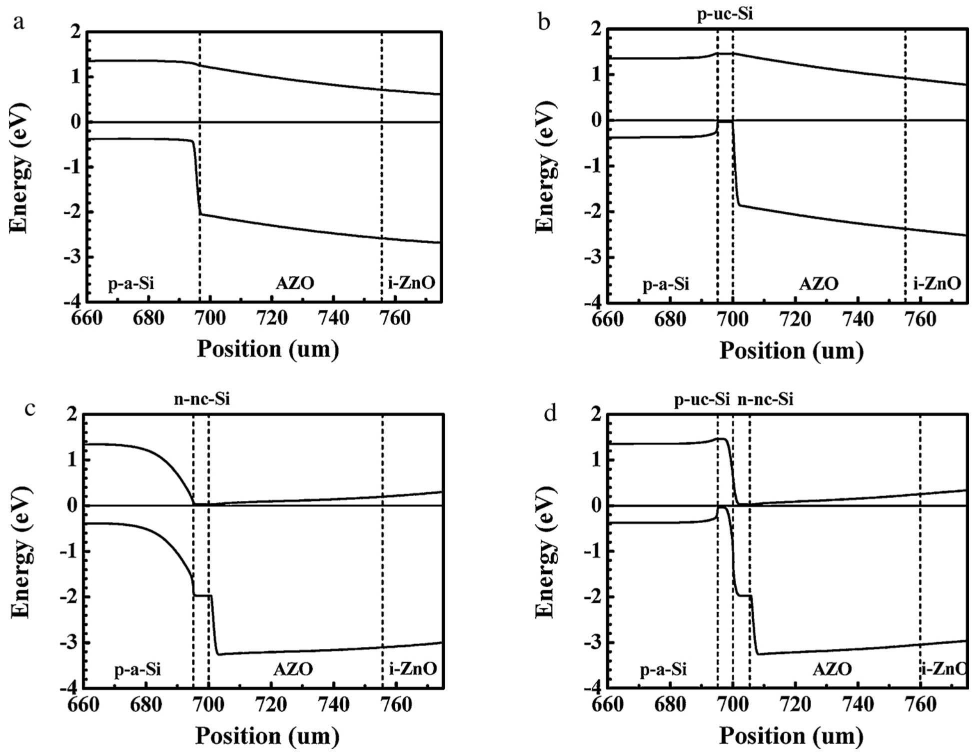

Fig. 5. Band diagrams for (a) the AZO TJ layer, (b) the p-uc-Si/AZO TJ layer, (c) the n-nc-Si/AZO TJ layer and (d) p-uc-Si/n-nc-Si/AZO TJ layer.

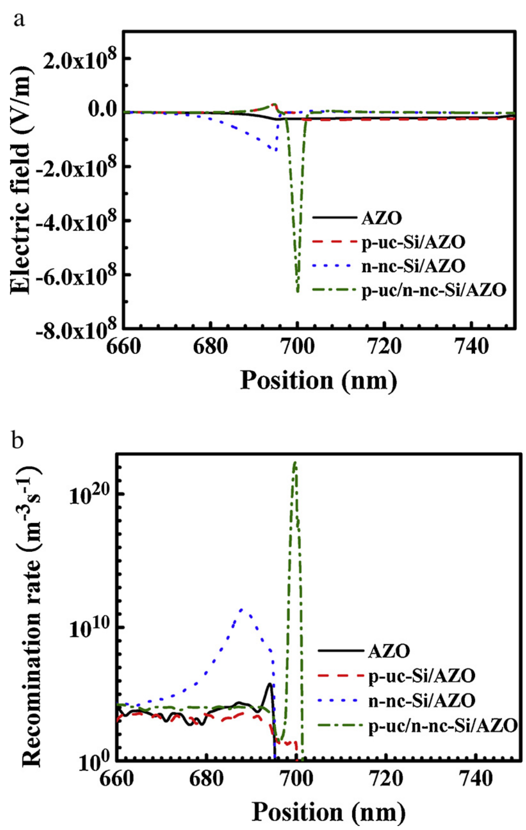

Fig. 6. (a) Electric field and (b) recombination rate around the TJ layer of a-Si:H/c-Si tandem solar cell for different TJ layers.

p-uc-Si and AZO (Fig. 5(b)). This caused the holes created in the top cell to accumulate, which results in a more rapid FF reduction. In the case of the n-nc-Si/AZO TJ layer, p/n junctions formed between p-a-Si:H and n-nc-Si and tunnel-recombination occurred sparsely (Fig. 5(c)). When p-uc-Si/n-nc-Si/AZO was used as a TJ layer, the holes and electrons were effectively tunnel-recombined between p-uc-Si and n-nc-Si (Fig. 5(d)). The changes in the band diagram were confirmed according to each TJ layer. The simulation results show how the electric field and the recombination rate vary according to the TJ layers used, as shown in Fig. 6. Fig. 6(a) shows the electric field of the tandem solar cells for the different TJ layers. In the case of the p-uc-Si/n-nc-Si/AZO TJ layers, the electric field is 7×10^8 V/m. The high electric field formed by the p/n junction accelerates the tunneling of the carrier at the center of the p/n junction. A low electric field can decrease the built-in voltage in the top cell and can drastically reduce V_{oc} and increase the series resistance in the tandem solar cell. For the TJ layer to function properly, the electric field must be above 10^8 V/m so that field-dependent tunneling occurs [20]. The recombination rates near the TJ layers are shown in Fig. 5(b). The recombination rate is over $10^{20}\,m^{-3}S^{-1}$ in the p-uc-Si/n-nc-Si/AZO TJ layers. It can be seen that the carriers formed on the top and bottom cells recombine at the TJ layers.

4. Conclusions

Tandem solar cells consisting of an a-Si:H top cell and a CIGS bottom cell were computationally examined using ASA simulations. First, a-Si:H solar cells with various optical bandgaps and a CIGS solar cell were simulated separately. Then, the current matching conditions the optical band gap control and thickness control were examined and optimization of TJ layer. The optimal tandem solar cell output parameter such as V_{oc} = 1.67 V, J_{sc} = 17.57 mA/cm^2, FF = 79.72% and Eff = 23.32%. Our numerical simulations closely approximate the performance of actual devices and would contribute to the fabrication of high efficiency a-Si:H/CIGS tandem solar cell.

Acknowledgements

This work was supported by the Korea Institute of Energy Technology Evaluation and Planning (KETEP) and the Ministry of Trade, Industry and Energy (MOTIE) of the Republic of (No. 20173010012940) and Basic Science Research Program through the National Research Foundation of Korea (NRF) funded by the Ministry of Science, ICT & Future Planning (NRF-2016R1C1B1011508).

References

[1] L. Mazzarella, A.B. Morales-Vilches, L. Korte, R. Schlatmann, B. Stannowski, Ultra-thin nanocrystalline n-type silicon oxide front contact layers for rear-emitter silicon heterojunction solar cells, Sol. Energy Mater. Sol. Cells 179 (2018) 386–391.
[2] J. Cho, S.M. Iftiquar, D.P. Pham, J. Jung, J. Park, S. Ahn, A.H.T. Le, J.S. Kim, J. Yi, Improvement in performance of tandem solar cell by applying buffer layer, back reflector and higher crystallinity of the microcrystalline Si active layer of bottom subcell, Thin Solid Films 639 (2017) 56–63.
[3] T. Kato, A. Handa, T. Yagioka, T. Matsuura, K. Yamamoto, S. Higashi, J.-L. Wu, K.F. Tai, H. Hiroi, T. Yoshiyama, T. Sakai, H. Sugimoto, Enhanced efficiency of Cd-free Cu(In,Ga)(Se,S)$_2$ minimodule via (Zn,Mg)O second buffer layer and alkali post treatment, 44th IEEE Photovoltaic Specialists Conference (2017).
[4] First Solar Press Release, First Solar Builds the Highest Efficiency Thin Film PV Cell on Record, (2014) 5 August.
[5] B.M. Kayes, H. Nie, R. Twist, S.G. Spruytte, F. Reinhardt, I.C. Kizilyalli, G.S. Higashi, 27.6% conversion efficiency, a new record for single junction solar cells under 1 sun illumination, Proceedings of the 37th IEEE Photovoltaic Specialists Conference, (2011).
[6] T. Matsui, H. Sai, T. Suezaki, M. Matsumoto, K. Saito, I. Yoshida, M. Kondo, Development of highly stable and efficient amorphous silicon based solar cells, 28th European Photovoltaic Solar Energy Conference and Exhibition, EU-PVSEC Proc. (2013), pp. 2213–2217.
[7] T. Matsui, K. Maejima, A. Bidiville, H. Sai, T. Koida, T. Suezaki, M. Matsumoto, K. Saito, I. Yoshida, M. Kondo, High-efficiency thin-film silicon solar cells realized by integrating stable a-Si:H absorbers into improved device design, J. Appl. Phys. 54 (2015) 08kb10.
[8] M. Boccard, M. Despeisse, J. Escarre, X. Niquille, G. Bugnon, S. Hanni, M. Bonnet-Eymard, F. Meillaud, C. Ballif, High-stable-efficiency tandem thin-film silicon solar cell with low-refractive-index silicon-oxide interlayer, IEEE J. Photovoltaics 4 (2014) 1368–1373.
[9] M.A. Green, K. Emery, Y. Hishikawa, W. Warta, E.D. Dunlop, Solar cell efficiency tables (version 46), Prog Photovoltaics Res Appl 23 (2015) 805–812.
[10] L.L. Kazmerski, Stability and Ternary Chalcopyrite Photovoltaic Devices, Natl Bur Stand Spec Publ, 1979, pp. 30–40.
[11] H. Saïdi, M.F. Boujmil, B. Durand, J.L. Lazzari, M. Bouaïcha, Elaboration and characterization of CuInSe2 thin films using one-step electrodeposition method on silicon substrate for photovoltaic application, Mater. Res. Express 5 (2018) 016414.
[12] M. Saifullah, J. Gwak, J.H. Park, S. Ahn, K. Kim, Y.J. Eo, J.H. Yun, Effect of substrate temperature during the three-stage process on the CuInSe2 solar cell characteristics, Curr. Appl. Phys. 17 (2017) 1194–1201.
[13] T. Nakada, S. Kijima, Y. Kuromiya, R. Arai, Y. Ishii, N. Kawamura, H. Ishizaki, N. Yamada, Chalcopyrite thin-film tandem solar cells with 1.5 V open-circuit-voltage, 2006 IEEE 4th World Conference on Photovoltaic Energy Conversion, WCPEC-4 (2007) 400–403.
[14] M. Elbar, S. Tobbeche, Numerical simulation of CGS/CIGS single and tandem thin-filmsolar cells using the Silvaco-Atlas software, Energy Procedia 74 (2015) 1220–1227.
[15] A. Guchhait, H.A. Dewi, S.W. Leow, H. Wang, G. Han, F.B. Suhaimi, S. Mhaisalkar, L.H. Wong, N. Mathews, Over 20% efficient CIGS – perovskite tandem solar cells, Energy Lett. 2 (2017) 807–812.
[16] C.Y. Tsai, C.Y. Tsai, Development of amorphous/microcrystalline silicon tandem thin-film solar modules with low output voltage, high energy yield, low light-induced degradation, and high damp-heat reliability, J. Nanomater. 2014 (2014) 861741.
[17] P.D. Paulson, R.W. Birkmire, W.N. Shafarman, Optical characterization of $CuIn_{1-x}Ga_xSe_2$ alloy thin films by spectroscopic ellipsometry, J. Appl. Phys. 94 (2003) 879–888.
[18] S. Ishizuka, A. Yamada, P.J. Fons, H. Shibata, S. Niki, Erratum: impact of a binary Ga_2Se_3 precursor on ternary $CuGaSe_2$ thin-film and solar cell device properties, Appl. Phys. Lett. 103 (2013) 269903.
[19] J.A.M. AbuShama, S. Johnston, T. Moriarty, G. Teeter, K. Ramanathan, R. Noufi, Properties of ZnO/CdS/CuInSe2 solar cells with improved performance, Prog. Photovoltaics Res. Appl. 12 (2004) 39–45.
[20] Q. Gu, A. Schiff, J.B. Chevrier, B. Equer, High-field electron-drift measurements and the mobility edge in hydrogenated amorphous silicon, Phys. Rev. B 52 (1995) 5696.